Optical-resolution photoacoustic microscopy based on two-dimensional scanning galvanometer

Yi Yuan, Sihua Yang, and Da Xing

Citation: Appl. Phys. Lett. **100**, 023702 (2012); doi: 10.1063/1.3675907
View online: http://dx.doi.org/10.1063/1.3675907
View Table of Contents: http://apl.aip.org/resource/1/APPLAB/v100/i2
Published by the American Institute of Physics.

Optical-resolution photoacoustic microscopy based on two-dimensional scanning galvanometer

Yi Yuan, Sihua Yang, and Da Xing[a)]
MOE Key Laboratory of Laser Life Science and Institute of Laser Life Science, College of Biophotonics, South China Normal University, Guangzhou, China

(Received 22 October 2011; accepted 19 December 2011; published online 9 January 2012)

An optical-resolution photoacoustic microscopy system was designed and fabricated by integration of a two-dimensional scanning galvanometer, an objective lens, an unfocused ultrasound transducer, and a sample stage. The lateral resolution of the system was measured to be ~500 nm. *Ex vivo* erythrocytes were used to test the imaging capability of the system, and a single erythrocyte was mapped with high contrast. Furthermore, *in vivo* blood vessels of a mouse ear were clearly shown, and the injured blood vessels were also monitored. The experimental results demonstrate that galvanometer-based photoacoustic microscopy holds clinical potential in detecting lesion of erythrocyte and blood vessel. © *2012 American Institute of Physics*. [doi:10.1063/1.3675907]

Photoacoustic (PA) imaging is a noninvasive imaging method with high acoustical resolution and high optical contrast.[1–3] When absorbers are irradiated by a time-resolved light, the absorption of light will result in a rapid thermoelastic expansion and cause a stress distribution to generate ultrasonic waves, which can be detected by a highly sensitive ultrasound transducer. Then, the detected PA signals can be reconstructed to demonstrate the optical absorption distribution within tissue.[4]

PA imaging has attracted considerable attention in recent years due to its excellent properties. Several PA imaging systems, such as PA rotating scan system with single-element transducer or sub-elements transducer,[5,6] PA microscopy,[7] PA imaging system based on Fresnel zone plate transducer,[8] intravascular PA imaging system, and PA imaging endoscope,[9,10] have been developed for imaging biological tissue. In addition, PA imaging has been applied in early detection of breast tumor,[11] noninvasive monitoring of cerebrovascular activities and blood oxygenation in small animals,[12] brain functional imaging,[13] monitoring of vascular damage during tumor photodynamic therapy,[14] and detection of differentiate atherosclerotic plaques.[15]

In this paper, we present an optical-resolution PA microscopy system for *in vivo* blood vessel imaging. It integrates a two-dimensional scanning galvanometer, an objective lens, an unfocused ultrasound transducer, and a sample stage. The lateral resolution of the PA microscopy is quantitatively analyzed to be ~500 nm. The PA image of erythrocytes *ex vivo* was reconstructed by the maximum amplitude projection algorithm,[7] and single erythrocyte was clearly distinguished. Normal and injured blood vessels of mouse ears were imaged *in vivo* with high resolution by the system.

The schematic of the experimental setup is shown in Fig. 1. An Nd:YAG laser, operating at the wavelength of 532 nm with a full-width at high magnitude (FWHM) of 10 ns and a repetition of 15 Hz, was used as the light source. The light, through a beam expander lens and a collimating lens, was scanned by a 2D scanning galvanometer (6231 H, Cambridge Technology). A field flattening lens with magnification of ×4 or ×40 was used as the objective lens. The light was focused by the objective lens to irradiate the tested sample. An unfocused ultrasound transducer with center frequency of 15 MHz and −6 dB bandwidth of 100% was used to receive the PA signals generated by the tested sample on the glass slide. The 2D scanning galvanometer, triggered by the signals of the pump laser, was controlled by a computer. The PA signals were recorded by the computer through the signal amplifier and a dual-channel data acquisition card. The sampling rate of the data acquisition card was 100 Msamples/s.

The lateral resolution of the PA microscopy was determined by the numerical aperture (NA) of the objective lens. In theory, the lateral resolution can be estimated by the formula: $0.51\lambda/\mathrm{NA}$. We used Au nanoparticles with a diameter of ~35 nm to evaluate the lateral resolution of the PA microscopy system. The NA of the objective lens with magnification of ×40 is ~0.65. A Gaussian amplitude fitting of the measured point spread function is shown in Fig. 2. The lateral resolution of the system, calculated by the FWHM of the point spread function, is ~500 nm, which is slightly larger than the theoretical value $0.51\lambda/\mathrm{NA} \approx 417$ nm.

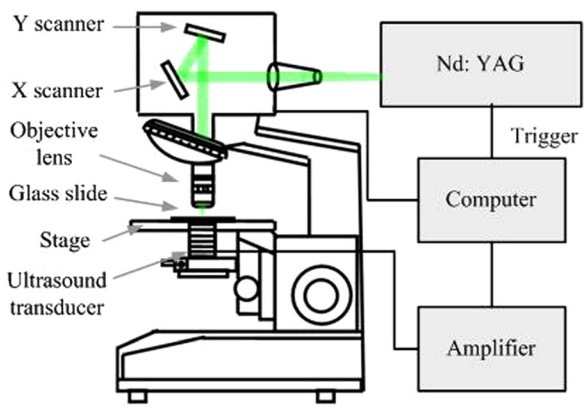

FIG. 1. (Color online) Schematic diagram of the PA microscopy.

[a)]Author to whom correspondence should be addressed. Electronic mail: xingda@scnu.edu.cn. Tel.: +86-20-85210089. Fax: +86-20-85216052.

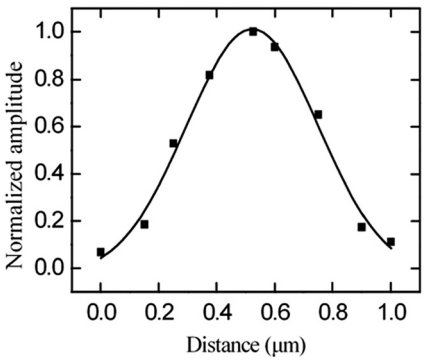

FIG. 2. Gaussian amplitude curve fitting of measured Au nanoparticles point spread function.

The PA microscopy system was used to image erythrocytes from a BALB/c mouse. A field flattening lens used for focusing light has the magnification of ×40. Fig. 3(a) is the reconstructed PA image of the erythrocytes. The single erythrocyte can be clearly distinguished. As the normal erythrocyte has the characteristics of thicker edge and thinner center, the contrast of the edge in the PA image of the erythrocyte in Fig. 3(a) is higher than that of the center. Fig. 3(b) is the reconstructed profile of the erythrocyte marked by the white dotted line in Fig. 3(a). The diameter of the erythrocyte is about 5 μm. The experimental result proves that the fabricated PA microscopy system is able to image erythrocytes and distinguish single erythrocyte.

The PA microscopy system was further applied in *in vivo* imaging blood vessels of a BALB/c mouse with body weight of 31 g. The fur of the mouse ear was shaven and chemically depilated before imaging. The skin was cleaned with 0.9% sodium chloride irrigation solution. General anesthesia (i.e., sodium pentobarbital, 40 mg/kg; supplemental, 10 mg/kg/h or as necessary) was applied to keep the mouse with no movement during the experiment. A field flattening lens with magnification of ×4 was used to scan a larger region. Fig. 4(a) is the reconstructed PA image of blood vessels of the mouse ear, and the structure of the blood vessels can be seen clearly. The diameter of one micro vessel pointed out with the arrow A is measured to be ~25 μm. Fig. 4(b) is the B-scan image in *x-z* plane from the dashed line in Fig. 4(a). Numbers 1–5 indicate the corresponded vessels between Figs. 4(a) and 4(b). The experimental result demonstrates that the PA microscopy is able to image the *in vivo* blood vessels with high resolution.

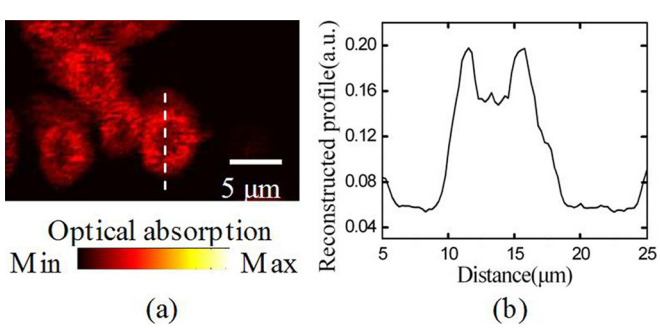

FIG. 3. (Color online) (a) Reconstructed PA image of the erythrocytes. (b) Reconstructed profile of erythrocyte marked by the white dotted line in (a).

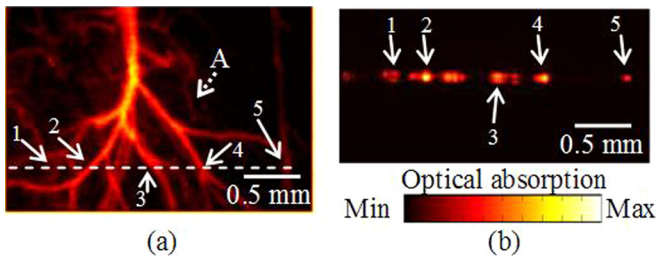

FIG. 4. (Color online) (a) Reconstructed PA image of the *in vivo* blood vessels of mouse ear. (b) B-scan image in the x-z plane at the position indicated by the dashed line in (a).

To further demonstrate the ability of the PA microscopy, we used the system to detect blood vessel injury of a BALB/c mouse *in vivo*. Fig. 5(a) is the reconstructed PA image of blood vessels of the mouse ear before the injury. The mouse was kept from moving after the first PA imaging, and the blood vessels in the imaging region were subsequently injured by the focused pulse laser with energy of 3 mJ. The reconstructed PA image of the injured blood vessels is shown in Fig. 5(b). Compared with Fig. 5(a), the morphology of the blood vessel in Fig. 5(b) pointed by arrow 1 has no change while that pointed by arrow 2 is changed. In order to quantitatively analyse the morphology changes of the blood vessels, the reconstructed profile of the blood vessels marked by the white dotted line in Figs. 5(a) and 5(b) was given in Fig. 5(c). The PA signal intensity at the position 1 in Fig. 5(b) was 25% lower than that of the same position in Fig. 5(a). The phenomena may be due to insufficient blood supply from the surrounding injured blood vessels. The diameter of the blood vessel at the position 2 in Fig. 5(a) is about 0.18 mm. Laser burn leads to blood vessels rupture and tissue congestion and finally forms a circular blood spot. The diameter of the blood spot is ~0.5 mm, and the area of the circular blood spot is ~0.2 mm^2. The intensity of the PA signal at the position 2 in Fig. 5(b) was~ two times higher than that of the

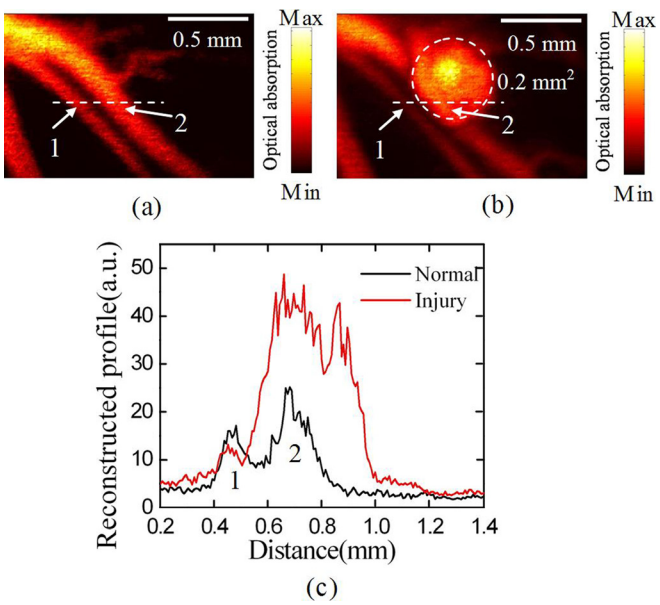

FIG. 5. (Color online) (a) Reconstructed PA images of the normal blood vessels of mouse ear. (b) Reconstructed PA images of the injured blood vessels of mouse ear. (c) Reconstructed profile of the blood vessel marked by the white dotted line in (a) and (b).

same position in Fig. 5(a), suggesting the optical absorption increased after the tissue congestion.

All above experimental results show that the PA images of biology tissues are reconstructed with the high resolution through the fabricated PA microscopy system. However, two aspects of the system need to be improved in the next work. First, the rate of the data acquisition was controlled by the repetition rate of the pulsed laser. Due to the limitation of the laser repetition rate, the system cannot accomplish real-time dynamic imaging and monitoring. A laser with repetition frequency of 24 Hz or higher is required to be used in the future. Second, the PA microscopy system works only in transmission mode. This limits its applications in the clinic. A system with a reflection-mode is under developing in our group.

In summary, we developed an optical-resolution PA microscopy system based on two-dimensional scanning galvanometer for *in vivo* imaging blood vessel. The lateral resolution was ~500 nm for Au nanoparticles imaging. *Ex vivo* single erythrocyte was distinguished with high contrast and high resolution. The normal and injured blood vessels were imaged clearly. All these demonstrate that the PA system has potential application in detecting inflammatory tissue of vascular structure and monitoring neovascularization in tumor angiogenesis.

This research is supported by the National Basic Research Program of China (2011CB910402; 2010CB732602), the Program for Changjiang Scholars and Innovative Research Team in University (IRT0829), and the National Natural Science Foundation of China (81127004, 11104087, 30870676).

[1]X. D. Wang, Y. J. Pang, G. Ku, X. Y. Xie, G. Stoica, and L. V. Wang, Nat. Biotechnol. **21**, 803 (2003).
[2]Y. G. Zeng, D. Xing, Y. Wang, B. Z. Yin, and Q. Chen, Opt. Lett. **2**, 1760 (2004).
[3]Z. Yuan, Q. Z. Zhang, and H. B. Jiang, Opt. Express **14**, 6749 (2006).
[4]D. W. Yang, D. Xing, H. M. Gu, Y. Tan, and L. M. Zeng, Appl. Phys. Lett. **87**, 194101 (2005).
[5]S. H. Yang, D. Xing, Y. Q. Lao, D. W. Yang, L. M. Zeng, L. Z. Xiang, and W. R. Chen, Appl. Phys. Lett. **90**, 243902 (2007).
[6]B. Z. Yin, D. Xing, Y. Wang, Y. G. Zeng, Y. Tan, and Q. Chen, Phys. Med. Biol. **49**, 1339 (2004).
[7]K. Maslov, G. Stoica, and L. H. Wang, Opt. Lett. **30**, 625 (2005).
[8]H. Wang, D. Xing, and L. Z. Xiang, J. Phys. D: Appl. Phys. **41**, 095111 (2008).
[9]S. Sethuraman, J. H. Amirian, S. H. Litovsky, R. W. Smalling, and S. Y. Emelianov, Opt. Express **15**, 16657 (2007).
[10]Y. Yuan, S. H. Yang, and D. Xing, Opt. Lett. **35**, 2266 (2010).
[11]S. A. Ermilov, T. Khamapirad, A. Conjusteau, M. H. Leonard, R. Lacewell, K. Mehta, T. Miller, and A. A. Oraevsky, J. Biomed. Opt. **14**, 024007 (2009).
[12]H. F. Zhang, K. Maslov, M. Sivaramakrishnan, G. Stoica, and L. V. Wang, Appl. Phys. Lett. **90**, 053901 (2007).
[13]S. H. Yang, D. Xing, Q. Zhou, L. Z. Xiang, and Y. Q. Lao, Med. Phys. **34**, 3294 (2007).
[14]L. Z. Xiang, D. Xing, H. M. Gu, D. W. Yang, S. H. Yang, and L. M. Zeng, J. Biomed. Opt. **12**, 014001 (2007).
[15]S. Sethuraman, J. H. Amirian, S. H. Litovsky, R. W. Smalling, and S. Y. Emelianov, Opt. Express **16**, 3362 (2008).